BOREAS An international journal of Quaternary research

Deglaciation of the Scandinavian Ice Sheet and a Younger Dryas ice cap in the outer Hardangerfjorden area, southwestern Norway

CARL REGNÉLL, JASON P. BRINER, HAFLIDI HAFLIDASON, JAN MANGERUD AND JOHN INGE SVENDSEN

BOREAS

Regnéll, C., Briner, J. P., Haflidason, H., Mangerud, J. & Svendsen. J. I.: Deglaciation of the Scandinavian Ice Sheet and a Younger Dryas ice cap in the outer Hardangerfjorden area, southwestern Norway. *Boreas*. https://doi.org/10.1111/bor.12568. ISSN 0300-9483.

Understanding past responses of ice sheets to climate change provides an important long-term context for observations of present day, and projected future, ice-sheet change. In this work, we reconstruct the deglaciation of the marine-terminating western margin of the Scandinavian Ice Sheet in the outer Hardangerfjorden area of southwestern Norway, following the Last Glacial Maximum (LGM) until the start of the Holocene. We base our interpretations on a combination of geomorphological mapping using high-resolution (LiDAR) terrain models, 68 new cosmogenic nuclide ^{10}Be exposure ages and radiocarbon-dated lake sediment cores, supported by the stratigraphic position of the 12.1 ka Vedde Ash. We show that even the highest mountain summits in the area (~1200–1400 m a.s.l.) were ice-covered during the LGM, thus settling debates concerning the Scandinavian Ice Sheet thickness in this region. These summits emerged as nunataqs through the ice sheet about 22–18 ka, potentially owing to upstream ice thinning caused by the break-up and retreat of the Norwegian Channel Ice Stream. Following the break-up of the Norwegian Channel Ice Stream, the ice margin seemingly stabilized at the outermost coast for 3500–5500 years before the mouth of Hardangerfjorden became ice free at *c*. 14.5 ka. Subsequently, during the Bølling and Allerød periods, the ice sheet retreated rapidly into the inner parts of Hardangerfjorden before a major ice sheet re-advance during the Younger Dryas. We identify and reconstruct a sizeable, independent ice cap on the Ulvanosa mountain massif during the Younger Dryas (YD), a massif that earlier was mapped as covered by the Scandinavian Ice Sheet during the YD. We also document ice-free areas that are more extensive than previously thought between Hardangerfjorden and Matersfjorden during the YD.

Carl Regnéll (carl.regnell@uib.no), Haflidi Haflidason, Jan Mangerud and John Inge Svendsen, Department of Earth Science, University of Bergen, PO Box 7803, NO-5020 Bergen, Norway and Bjerknes Centre for Climate Research, Bergen, Norway; Jason P. Briner, Department of Geology, University at Buffalo, Buffalo, NY 14260, USA; *received 20th April 2021, accepted 9th October 2021.*

The complex topography of the dissected fjord landscape in southwestern Norway bears a close resemblance to the coastal fjord regions at the margins of the modern-day Greenland Ice Sheet. Establishing the timing and pattern of the last deglaciation in southwestern Norway is, therefore, valuable to contextualize predictions of future ice-sheet change under projected climate scenarios. However, the main motivation for this study is to describe and understand the glaciation history of this part of Norway.

During the Last Glacial Maximum (LGM), *c*. 26.5–19 ka (Clark *et al*. 2009), the Scandinavian Ice Sheet was connected to the British–Irish Ice Sheet across the North Sea (Fig. 1) and the Norwegian Channel Ice Stream flowed northwards along the west coast of Norway (Fig. 2). The ice stream subsequently broke up at *c*. 19–18 ka (Lehman *et al*. 1991; Sejrup *et al*. 1994, 2016; King *et al*. 1998; Morén *et al*. 2018), after which the western margin of the Scandinavian Ice Sheet became more or less parallel with the Norwegian coastline (Mangerud *et al*. 2017). ^{10}Be exposure dates from Utsira and southern Karmøy (Fig. 2A) suggest a retreat of the ice stream as early as 20 ka (Svendsen *et al*. 2015), but Briner *et al*. (2016) proposed that this apparent age is slightly too high owing to the inheritance of muon-produced ^{10}Be. Still, a tip of the southernmost part of western Norway apparently became ice free as early as about 18 ka (Vasskog *et al*. 2019), followed by ice-margin retreat in Boknafjorden beginning prior to 16 ka (Fig. 2A) (Gump *et al*. 2017). This early retreat contrasts with deglaciation around the mouth of Hardangerfjorden and further north, which did not become ice free until about 15 ka (Mangerud *et al*. 2013, 2016, 2017).

Following deglaciation of the outermost coast at *c*. 15 ka, the ice-sheet margin in the Hardangerfjorden area experienced a net retreat of >100 km (Fig. 2A) during the Bølling and Allerød warm periods (Mangerud *et al*. 2016). This period was apparently interrupted by an ice-sheet re-advance coinciding with the Older Dryas cold period at *c*. 14 ka, as inferred from radiocarbon-dated shell-bearing tills (Mangerud *et al*. 2016). From its restricted Allerød extent in inner Hardangerfjorden, the ice sheet re-advanced about 60 km to the island of Halsnøy in outer Hardangerfjorden during the Younger Dryas (hereafter YD) (Fig. 2A). The re-advance is documented by radiocarbon-dated shell-bearing tills and lake sediment records (Mangerud *et al*. 2016). The change from falling to rising relative sea level in a well-

DOI 10.1111/bor.12568

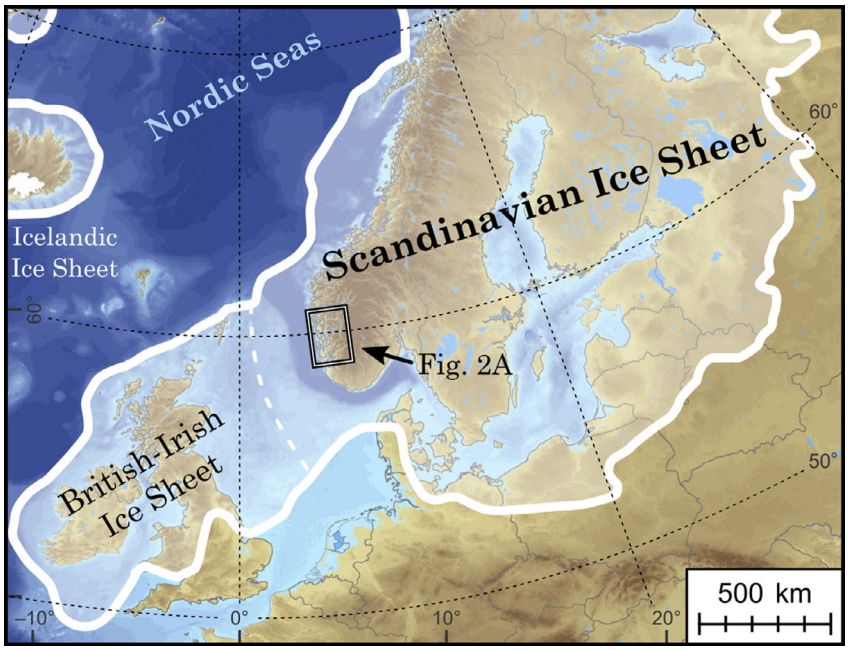

Fig. 1. Location of the study area (Fig. 2A) and the maximum ice-sheet extents (Last Glacial Maximum, LGM) during the last glacial period in northwestern Europe (modified from Hughes *et al*. 2016).

dated sea-level curve indicates that the re-advance started as early as 13.6 ka, i.e. in middle Allerød (Lohne *et al*. 2007). The culmination of the ice-sheet re-advance in the Hardangerfjorden area is dated to the end of the YD at 11.8 ka and the start of its subsequent retreat from this position to 11.6 ka (Lohne *et al*. 2012). In the early Holocene, the ice sheet then retreated about 120 km to the head of Hardangerfjorden in only *c*. 500 years, i.e. a retreat rate of ~240 m a^{-1} (Mangerud *et al*. 2013; Åkesson *et al*. 2020).

Whilst a wealth of previous research has dealt with the timing and configuration of the Allerød–YD ice-sheet re-advance in Hardangerfjorden, the more detailed geometry of the YD ice-sheet extent between Hardangerfjorden and Matersfjorden (Figs 2A, 3) still remains uncertain. Further, there are only limited chronological constraints on the deglaciation from the outer coast prior to the YD and no regional constraints on the ice thickness during the LGM and subsequent thinning during deglaciation. It has in fact long been debated whether the highest summits in Norway, including in this area, were ice covered or ice free during the LGM (e.g. Nesje *et al*. 1987, 1988; Follestad 1990; Nesje & Dahl 1990; Sollid & Sørbel 1994; Brook *et al*. 1996; Fjeldskaar 2000; Diesen 2003; Goehring *et al*. 2008). In this study, we use geomorphological mapping based on high-resolution Light Detection and Ranging (LiDAR) data combined with cosmogenic nuclide ^{10}Be exposure dating to resolve this problem in our study area.

In addition, we use lake sediment cores, dated by accelerator mass spectrometry (AMS) ^{14}C and the stratigraphic position of the 12.1 ka Vedde Ash (Mangerud *et al*. 1984; Lohne *et al*. 2013, 2014), to: (i) resolve whether the highest mountain peaks in the Hardangerfjorden area remained ice free or not during the LGM, and if not, date when they protruded as nunataqs and reconstruct the subsequent thinning history of the ice sheet; (ii) define the extent of the YD ice sheet between Hardangerfjorden and Matersfjorden; and (iii) identify if there were any independent ice caps in the higher mountain massifs during the YD.

Study area

Hardangerfjorden, the second-longest fjord in Norway, is more than 1000 m deep if all of the Holocene sediments are removed (Holtedahl 1975; Aarseth 1997) and it is bordered by steep mountains ranging from ~500 m a.s.l., around the mouth of the fjord, to ~1800 m a. s. l. near the head of the fjord. Across the outer part of the fjord lies the prominent Halsnøy moraine (Fig. 3), deposited by the Scandinavian Ice Sheet during the YD (e.g. Undås, 1963; Holtedahl 1967; Follestad 1972; Mangerud 2000; Lohne *et al*. 2012; Mangerud *et al*. 2013).

In this study, we focus on the mountains of Melderskind, Laurdalstind, Solfjell, Englafjell and Ulvanosa (Fig. 3), as well as the lower mountain Siggjo (474 m a.s.l.) on the island of Bømlo at the mouth of Hardangerfjorden (Fig. 2A). We also investigate lower-lying areas between Hardangerfjorden and Matersfjorden.

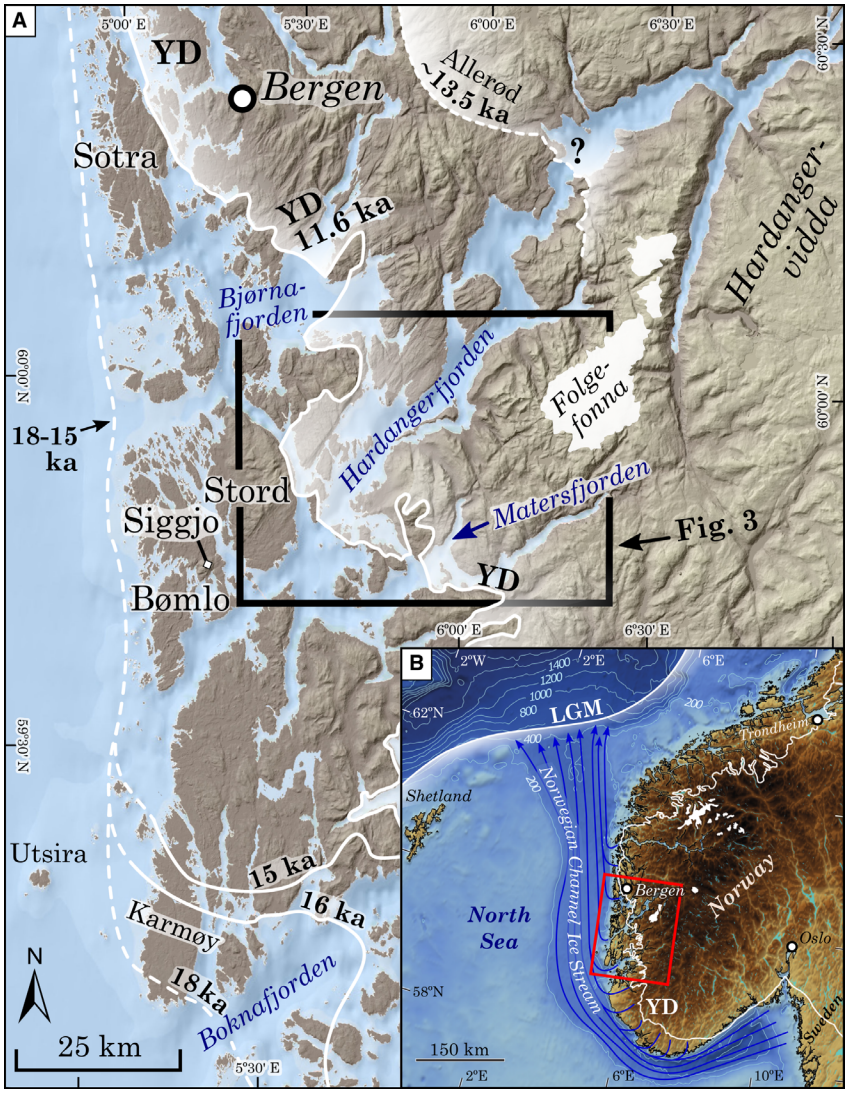

Fig. 2. A. Location map (boxes in Figs 1 and 2B) of areas discussed in the text. Ice margins are shown as white lines with ages in cal. ka BP (based on Anundsen 1972; Follestad 1972; Mangerud *et al.* 2016, 2017; Gump *et al.* 2017). B. Map of southern Norway and the adjacent North Sea showing the LGM ice margin and corresponding ice flow of the Norwegian Channel Ice Stream. The Younger Dryas (YD) ice margin (thin white line) is also shown (modified from Mangerud *et al.* 2013).

Material and methods

LiDAR and field mapping

The area was analysed for ice-marginal landforms on digital terrain models (DTMs) derived from LiDAR data compiled by the Norwegian Mapping Authority (https://hoydedata.no/LaserInnsyn/). From the DTMs, altitudes can be determined with a precision of <10 cm, relative to the Norwegian Normal zero (NN2000), in practice mean sea level. The remote sensing was complemented by ground truthing in the field.

Cosmogenic ^{10}Be exposure dating

To constrain the deglacial history we used cosmogenic ^{10}Be exposure dating of glacial erratic boulders ($n = 66$) and bedrock surfaces ($n = 2$). As the ice surface is expected to have thinned upstream during the retreat of the ice margin, we have collected rock samples on summits along Hardangerfjorden in order to date when they first protruded through the ice surface. These data are in turn used to reconstruct ice-sheet profiles along Hardangerfjorden during the deglaciation.

The rock samples were collected from the uppermost surfaces of large erratic boulders and exposed bedrock

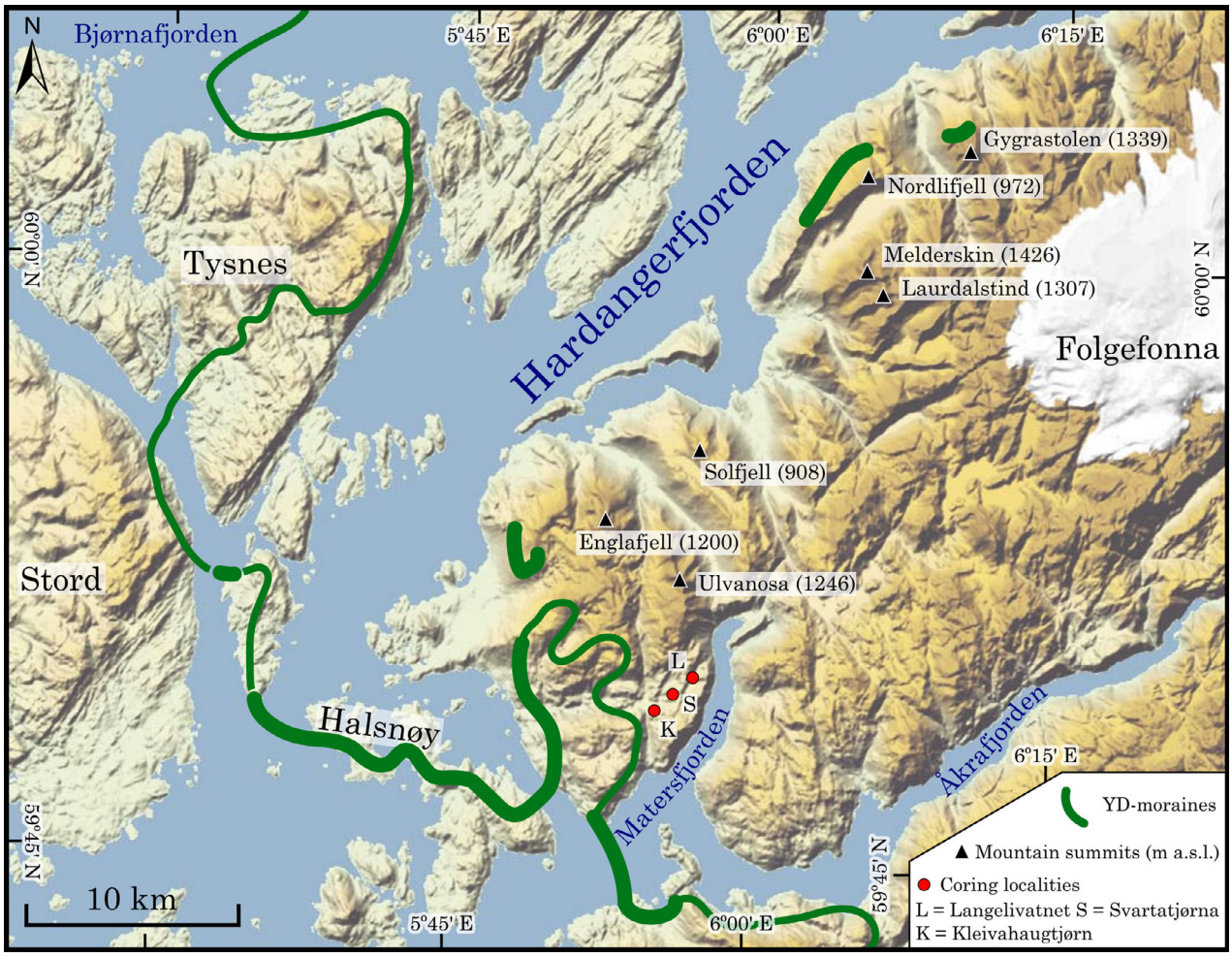

Fig. 3. Location map of outer Hardangerfjorden (location in Fig. 2A). Mountain summits mentioned in the text and coring location are marked. The YD ice margin is based on Follestad (1972) and Mangerud *et al.* (2016); note that our study will modify this ice margin between Hardangerfjorden and Matersfjorden (Fig. 6).

surfaces using a portable diamond saw, hammer and chisel. We sampled mostly flat surfaces and avoided edges. All of the samples were collected from above the local marine limit. Sample coordinates were determined using a handheld GPS and the elevations were later determined from the LiDAR DTMs. As many of the highest summits are covered with blockfields (Fig. 4), extra caution was taken to only sample large boulders perched on top of the blockfields in positions that were best explained by glacial transport and deposition (Fig. 4B).

All samples were prepared for ^{10}Be analysis at the University at Buffalo Cosmogenic Nuclide Laboratory. After the samples had been crushed and sieved and the quartz isolated, the samples were digested, and beryllium was isolated following procedures described in Young *et al.* (2013). ^{10}Be/^{9}Be ratios were measured at the Center for Mass Spectrometry, Lawrence Livermore National Laboratory, and normalized to standard 07KNSTD3110 with a reported ratio of 2.85×10^{-12} (Nishiizumi *et al.* 2007; Rood *et al.* 2010). Procedural blank ratios range from 1.1×10^{-15} to 3.9×10^{-15}, equating to background corrections of 1–4% of the sample total.

All ^{10}Be ages were calculated using version 3 of the online CRONUS Earth exposure age calculator (hess.ess.washington.edu; Balco *et al.* 2008; Balco 2017) using the regionally constrained production rate for Scandinavia of 4.13 ± 0.11 at g^{-1} a^{-1} (Stroeven *et al.* 2015; close to the locally determined production rate (4.15 ± 0.15 at g^{-1} a^{-1}) of Goehring *et al.* 2012a, b), and time-dependent (Lm) scaling (Lal 1991). We also note that if, instead of the Scandinavian production rate (Stroeven *et al.* 2015), we used the global 'primary' ^{10}Be production rate by Borchers *et al.* (2015), the ages would only be ~1% younger. Reported age uncertainties reflect the one sigma AMS analytical uncertainty. Ages refer to the sampling year (AD 2015–2017). We assume an erosion rate of 1.72×10^{-4} cm a^{-1} for all samples based on differential quartz vein relief observed on erratic

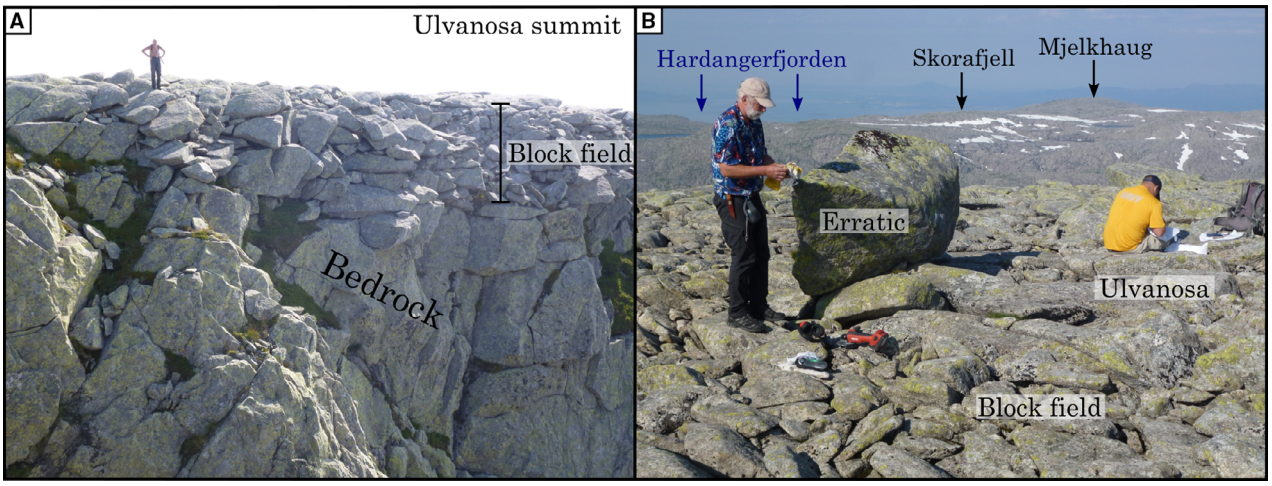

Fig. 4. A. Cross-section through a blockfield on top of Ulvanosa 1246 m a. s. l. Person for scale. B. Example of a boulder perched on top of the blockfield close to the summit of Ulvanosa. We, therefore, consider it as transported and deposited by the ice sheet, even though the rock type is similar to the local bedrock.

boulders at the Halsnøy moraine, outer Hardangerfjorden (Goehring *et al*. 2012a). We made no corrections for shielding by snow cover.

Elevation changes, owing to isostatic rebound, during a rock surface's exposure history will result in a time-varying rate of ^{10}Be production at the sampling site. The Marine Limit is 80 m a. s. l. near the Dyrrinda moraine, and thus the samples exposed at 11.6 ka BP are now located 70 m higher relative to sea level. Sample elevations can potentially be corrected for this using regional sea-level curves (e.g. Jones *et al*. 2019) and to exemplify the impact of using different elevations when calculating ^{10}Be ages we use sample 96-BM3 from the Dyrrinda moraine, for which we obtain a value of 12.2±0.3 ka. If instead we used an altitude 80 m lower (the YD relative sea level for the sample site), the age would be 13.1±0.3 ka. However, the isostatic uplift here was very fast during the first period and thus a 25 m lowering would probably be a more realistic 'mean' altitude, giving 12.4±0.3 ka. Nevertheless, atmospheric variability at the sampling sites, such as varying proximity to the ice margin, may counteract the effects of isostatic rebound on ^{10}Be production rates (Staiger *et al*. 2007). Our ^{10}Be ages are, therefore, calculated applying the current altitude of the samples.

Sediment coring, bathymetric and seismic surveying

Glacier-fed lake sediment records can be used to determine fluctuations of glacier and ice-sheet margins as glaciolacustrine sediments can often be distinguished from other lacustrine sediments (e.g. Mangerud *et al*. 1979; Lohne *et al*. 2012). In this study, two palaeolakes, Svartatjørna (314 m a.s.l.) and Kleivahaugtjørn (240 m a.s.l.) (Fig. 3), which are now partly mires, were cored using a 10-cm-diameter Russian peat corer. Lake Langelivatnet (Fig. 3) was cored using a modified Nesje piston corer (Nesje 1992). The cores were brought back to the University of Bergen and stored at ~4 °C before further sediment logging and laboratory analyses. A bathymetric survey of Langelivatnet was performed using a Lowrance Elite-5 HDI echo sounder, and a bathymetry map was produced in the software Reefmaster. The sedimentary infill of Langelivatnet was mapped with a portable EdgeTech 3100P chirp system and the seismic stratigraphy visualized using EdgeTech software.

Radiocarbon dating and identification of the Vedde Ash

The sediment cores were sampled at selected intervals for AMS ^{14}C dating, and the samples were sieved through 100- and 63-µm sieves before organic macrofossils were picked by tweezer under a light microscope. Although terrestrial material was preferred, some samples only contained fragmented macrofossils and it was therefore impossible to determine if they were all from terrestrial plants. Bulk sediment samples were dated where no macrofossils were found. The macrofossils were dried at 50°C and placed in sterilized and sealed vials before they were sent to the Radiocarbon Dating Laboratory at Lund University, Sweden, for AMS ^{14}C dating. All ^{14}C ages were calibrated using the IntCal20 calibration curve (Reimer, 2020) and are reported relative to AD 1950 (cal. a BP).

In addition, the core chronologies were also supported by the occurrence of the YD-age (12.1 cal. ka BP) Vedde Ash (Mangerud *et al*. 1984), based on its characteristic shard morphology and colours, the fact that it contains both the rhyolitic and basaltic components (Mangerud *et al*. 1984), its stratigraphic position and the fact that the Vedde Ash is the only visible ash layer found in western Norway (e.g. Lohne *et al*. 2012).

Table 1. ^{10}Be sample data and ages. All samples have a rock density of 2.65 g cm^{-3}.

Sample	Sample type	Latitude (°N)	Longitude (°E)	Elevation (m a.s.l.)	Sample thickness (cm)	Topographic shielding factor	^{10}Be concentration (at g^{-1})	^{10}Be age (ka)[1]
Siggjo								
14NOR-55	Boulder	59.747873	5.29469	467	1	1	41 645±1039	6.1±0.2
14NOR-56	Boulder	59.748824	5.29546	462	2	0.9903	96 783±1887	14.7±0.3
14NOR-57	Boulder	59.749069	5.29640	470	1	1	97 294±1824	14.4±0.3
Siggjo-1	Boulder	59.74931	5.29802	420	2	1	94 114±1791	14.8±0.3
78-Siggjo-2	Boulder	59.74842	5.29733	459	3.5	1	93 335±1793	14.3±0.3
Mjelkhaug								
81-UN53	Boulder	59.86258	5.85370	997	1	1	159 285±3013	14.9±0.3
Skorafjell								
82-UN55A	Boulder	59.86477	5.87675	1001	2	1	126 441±2568	11.8±0.2
82-UN56	Boulder	59.86191	5.87849	1003	1.3	1	129 514±2030	12.0±0.2
Englafjell								
65-14NOR-40	Boulder	59.89564	5.87827	1171	2	1	494 043±6579	41.9±0.6
65-14NOR-42	Boulder	59.89471	5.88078	1153	2	1	602 720±6658	52.8±0.6
Ulvanosa summit								
65-14NOR-31	Boulder	59.87263	5.94073	1187	2	1	26 8481±4986	21.8±0.4
65-14NOR-33	Boulder	59.86684	5.94333	1150	2	1	412 405±11 969	35.2±1.1
65-14NOR-36	Boulder	59.86738	5.93912	1109	2	0.99	294 113±5483	25.9±0.5
68-14NOR-32	Bedrock	59.87268	5.94072	1187	2	1	873 000±12 700	77.3±1.3
68-14NOR-38	Bedrock	59.87549	5.93476	1231	2	1	16 000 00±23 300	153.9±2.9
81-UN32	Boulder	59.86393	5.94030	1113	1.5	1	254 527±3749	21.9±0.3
81-UN33	Boulder	59.86435	5.94005	1111	1.4	1	211 543±3977	18.1±0.4
Solfjell								
SF1	Boulder	59.93310	5.94193	827	2	1	134 089±2513	14.6±0.3
SF2	Boulder	59.93360	5.94168	825	2	1	129 607±2755	14.1±0.3
SF3	Boulder	59.93360	5.94168	825	2	1	101 686±1915	11.0±0.2
SF4	Boulder	59.931877	5.94264	812	2	1	139 411±2619	15.4±0.3
SF5	Boulder	59.931734	5.94273	810	2	1	128 833±2430	14.2±0.3
SF6	Boulder	59.931406	5.94273	807	2	1	129 254±2108	14.3±0.2
Melderskin								
86-M57	Boulder	60.00284	6.06856	1332	2.4	1	1 652 382±18 595	144.8±2.1
86-M58	Boulder	60.00299	6.06933	1326	2.2	1	1 295 300±17 243	107.5±1.7
86-M59	Boulder	60.00309	6.06945	1330	1.7	1	251 375±7001	18.0±0.5
86-M60	Boulder	60.00708	6.08230	1421	1.9	1	322 154±4658	21.6±0.3
Laurdalstind								
86-M61	Boulder	59.99479	6.08192	1304	2.4	1	457 769±5964	34.5±0.5
86-M62	Boulder	59.99471	6.08243	1305	1.8	1	381 027±5721	28.3±0.4
Ulvanosa vertical transect								
81-UN34	Boulder	59.86741	5.93622	1091	1.6	1	155 593±2929	13.5±0.3
81-UN35	Boulder	59.86658	5.93249	1067	1.7	1	145 153±2948	12.8±0.3
81-UN36	Boulder	59.86658	5.93143	1060	1.1	1	140 356±2343	12.4±0.2
81-UN37	Boulder	59.8669	5.93127	1059	1.4	1	149 930±2841	13.3±0.3
81-UN38	Boulder	59.86624	5.92077	1033	1	1	137 898±3490	12.4±0.3
81-UN39	Boulder	59.86406	5.92770	1008	1.4	1	131 691±2904	12.2±0.3
82-UN40	Boulder	59.85796	5.91997	857	1.4	1	119 979±3456	12.6±0.4
82-UN41	Boulder	59.85829	5.91544	871	1.6	1	113 157±2277	11.8±0.2
82-UN42	Boulder	59.85804	5.91970	875	1.5	1	111 316±2676	11.5±0.3
82-UN43	Boulder	59.85658	5.92050	867	1.4	1	123 247±2305	12.9±0.2
82-UN44	Boulder	59.85176	5.91913	825	1.2	1	135 669±2208	14.7±0.2
82-UN45	Boulder	59.84882	5.92008	768	1.3	1	133 033±2526	15.2±0.3
85-UN46	Boulder	59.84719	5.92179	770	1.1	1	123 385±5134	14.0±0.6
85-UN47	Boulder	59.8473	5.92143	771	2	1	150 489±2938	17.3±0.3
85-UN48	Boulder	59.84097	5.92219	662	1.5	1	114 584±2187	14.4±0.3
85-UN49	Boulder	59.84081	5.92456	677	1.4	1	114 447±1984	14.1±0.3
85-UN50	Boulder	59.83998	5.92484	667	1.9	1	109 787±3132	13.7±0.4

(continued)

Table 1. (continued)

Sample	Sample type	Latitude (°N)	Longitude (°E)	Elevation (m a.s.l.)	Sample thickness (cm)	Topographic shielding factor	^{10}Be concentration (at g^{-1})	^{10}Be age (ka)[1]
85-UN51	Boulder	59.83941	5.91997	613	1.9	1	104 060±2428	13.7±0.3
85-UN52	Boulder	59.83941	5.91997	613	1.7	1	109 000±3119	14.3±0.4
Dyrrinda moraine								
96-BM1	Boulder	59.84025	5.91625	580	2	1	105 968±2346	14.4±0.3
96-BM2	Boulder	59.83982	5.91644	580	2	1	78 066±1667	10.5±0.2
96-BM3	Boulder	59.83971	5.91636	580	2	1	90 048±2032	12.2±0.3
96-BM4	Boulder	59.83862	5.91592	560	2	1	85 409±1798	11.7±0.3
96-BM5	Boulder	59.81718	5.91191	240	2	1	60 695±1227	11.3±0.2
96-BM6	Boulder	59.81678	5.91304	215	2	1	59 113±1137	11.3±0.2
Sandhaugene and Langhaugene moraines								
96-SH1	Boulder	59.93263	5.92615	577	2	1	91 127±2155	12.3±0.3
96-SH2	Boulder	59.93289	5.92758	575	2	1	85 660±1624	11.6±0.2
96-SH3	Boulder	59.93292	5.92782	575	2	1	82 880±1574	11.2±0.2
96-SH4	Boulder	59.92870	5.93236	607	2	1	93 897±1907	12.4±0.3
96-SH5	Boulder	59.92870	5.93236	607	2	1	57 929±1115	7.6±0.1
97-SH6	Boulder	59.92831	5.93154	600	2	1	88 507±1756	11.7±0.2
97-SH7	Boulder	59.92839	5.93107	600	2	1	85 372±3629	11.3±0.5
97-SH8	Boulder	59.92839	5.93107	600	2	1	84 755±1694	11.2±0.2
97-SH9	Boulder	59.929969	5.93053	610	2	1	87 264±1657	11.5±0.2
99-SH10	Boulder	59.929969	5.93053	610	2	1	87 137±2535	11.4±0.3
97-SH11	Boulder	59.93029	5.92934	600	2	1	92 366±1747	12.2±0.2
97-SH12	Boulder	59.93140	5.91934	545	2	1	82 523±1626	11.5±0.2
97-SH13	Boulder	59.93140	5.91934	545	2	1	85 323±2455	11.9±0.3
97-SH14	Boulder	59.93173	5.91893	542	2	1	85 610±1631	12.0±0.2

[1]Scandinavian production rate (Stroeven *et al.* 2015).

Results

Cosmogenic ^{10}Be exposure dating results

To date the retreat and thinning of the ice sheet, 66 boulders and two bedrock samples were dated (Table 1). Samples were collected from the mountains of Ulvanosa, Melderskin and Laurdalstind in the east (previously mapped as being above the YD ice-sheet surface; Follestad 1972) and the island of Bømlo (previously mapped as being beyond the YD limit; Follestad 1972) on the outer coast to the west (Figs 2A, 3).

Exposure ages from the highest peaks and the outer coast. – The oldest ^{10}Be exposure ages were obtained from areas above 1100 m a. s. l. on the mountain summits of Englafjell, Ulvanosa, Melderskind and Laurdalstind (Figs 5,6). The ages displayed a large

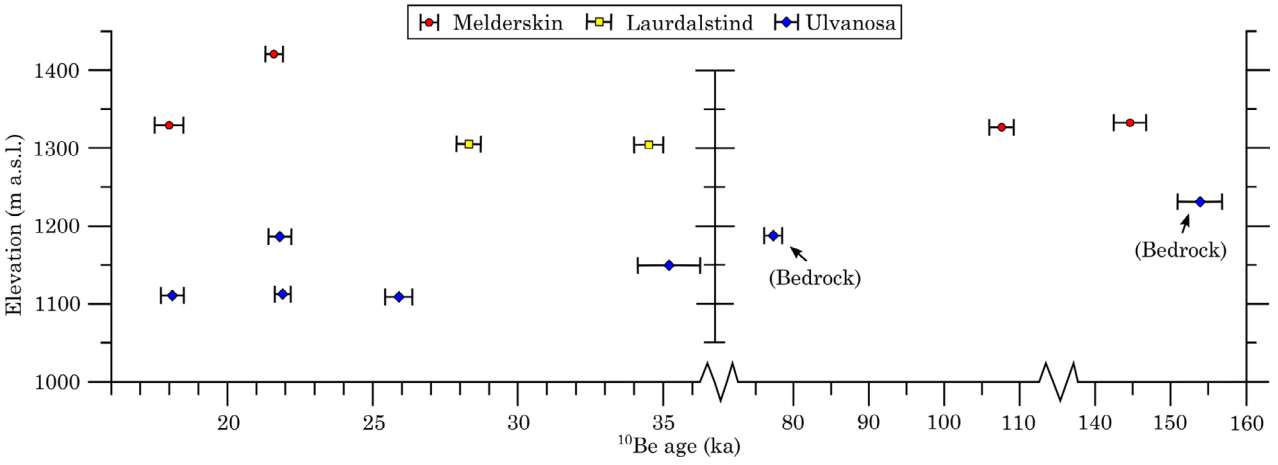

Fig. 5. ^{10}Be ages of boulders from the summits of Melderskin (1426 m a.s.l.), Laurdalstind (1307 m a.s.l.) and Ulvanosa (1246 m a.s.l.) plotted against elevation. Note that the two older ages from Ulvanosa are bedrock samples and the two breaks in the time scale at 36–75 and 115–140 ka. Note also that there are samples younger than 22 ka on both Melderskin and Ulvanosa.

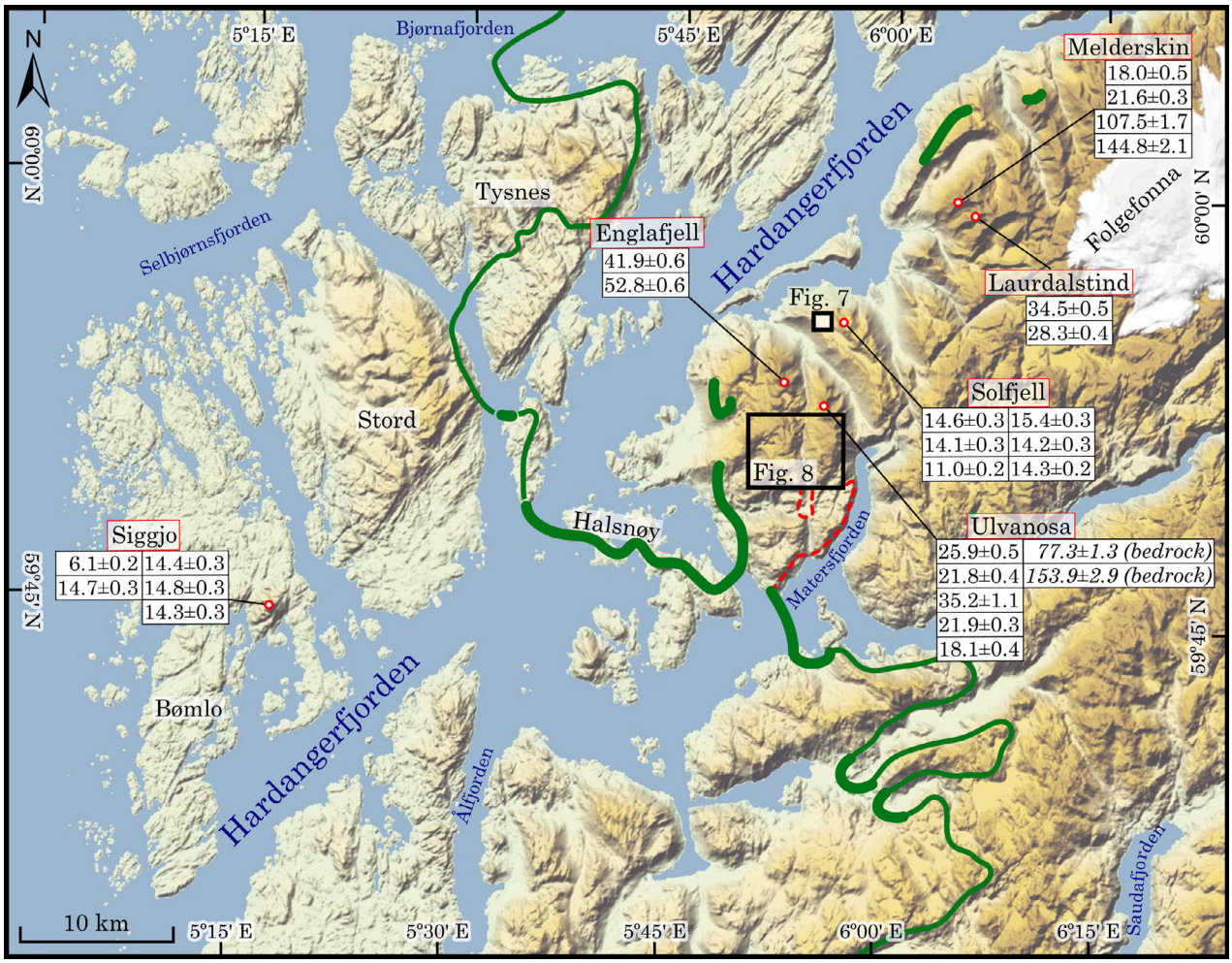

Fig. 6. Location map with ^{10}Be ages from summits around Hardangerfjorden. YD ice margins (green lines) after Mangerud *et al.* (2016) and Gump *et al.* (2017). Note that, based on our results in this study, we have modified the ice margin between Ulvanosa and Matersfjorden (dashed red line) as compared with the previous work by Follestad (1972) (Fig. 3), and we have reconstructed a local ice cap on the Ulvanosa massif (Fig. 14).

scatter with four ages as old as 155–75 ka and the remaining nine between 35 and 18 ka.

All ^{10}Be samples from the summit of mount Siggio on the western coast yielded ages between 14.3 and 14.8 ka (average = 14.5 ka), after removal of an outlier of 6.1 ka (Fig. 6).

On the western slope of Solfjell, farther into Hardangerfjorden, lie two conspicuous and parallel moraine ridges called Langhaugene and Sandhaugene, at 560–620 m a.s.l. (Fig. 7). From their appearance, it is difficult to tell whether they are lateral moraines and, if so, whether they were deposited by ice from the north or south. We dated 14 boulders from the moraines and surroundings (Fig. 7). All but one span 12.4–11.2 ka (average = 11.7 ka), indicating that the moraines were emplaced during the YD between ice flowing from both the north and the south.

Above the Langhaugene and Sandhaugene moraines, at 807–827 m a. s. l. on Solfjell, ^{10}Be ages from six erratic boulders fell between *c.* 14.1 and 15.5 ka and one boulder gave a value of 11 ka (Fig. 6).

Vertical transect of exposure ages on Ulvanosa mountain. – To address the regional thinning history of the ice sheet, 19 boulders were sampled in a vertical transect from 1091 to 613 m a. s. l. on the southern slope of Ulvanosa mountain (Fig. 8). The resulting ages range from 17.3 to 11.5 ka, with older ages at lower elevations than on higher ground (Fig. 9). Surprisingly, even the lowest samples yielded pre-YD ages (13.7–14.4 ka) even though they are located well inside the YD ice extent as mapped by Follestad (1972) (Fig. 3), indicating that larger areas remained ice free during the YD than previously thought.

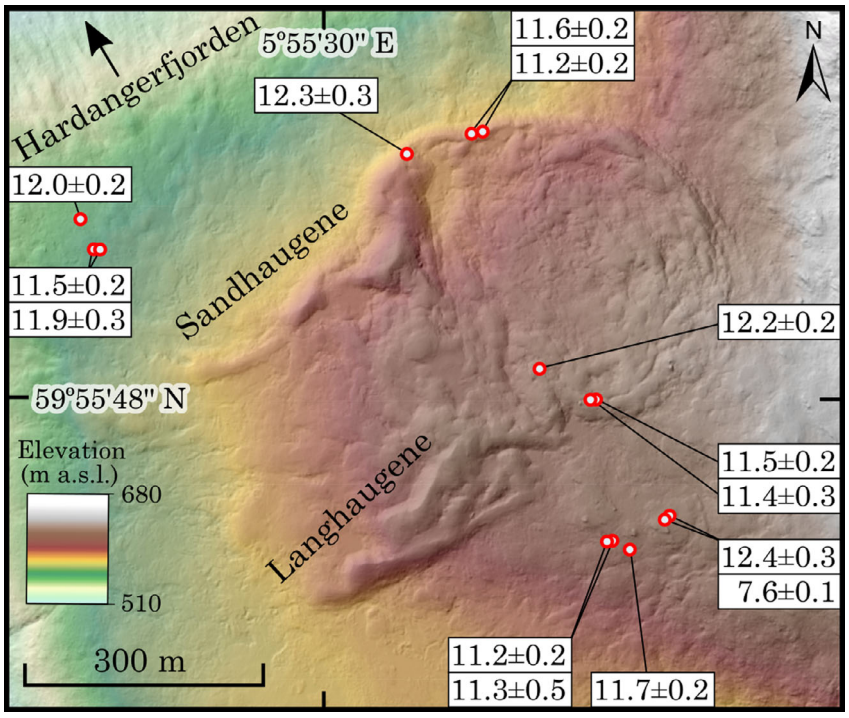

Fig. 7. LiDAR DTM with ^{10}Be ages from Sandhaugene and Langhaugene moraines (location in Fig. 6).

Exposure ages from the Dyrrinda moraine and mapping of terraces in Tveitedalen. – Our ^{10}Be ages from just outside the Dyrrinda moraine (Figs 8,10) suggest pre-YD ages, contrary to earlier interpretations, in which this area was covered by YD ice (Follestad 1972). We therefore decided to also sample the Dyrrinda moraine for exposure dating.

From the LiDAR-DTMs we identified a lobate continuation of the Dyrrinda moraine south of Bergsdalen (Fig. 10). Two boulder samples were collected

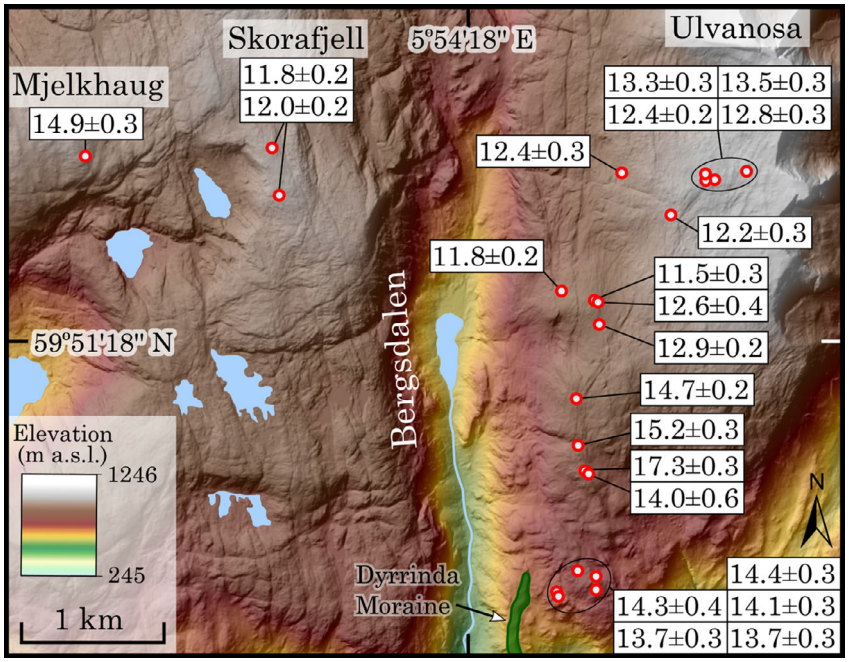

Fig. 8. LiDAR DTM with ^{10}Be ages from lower altitudes on the Ulvanosa massif (location in Fig. 6). Note the Dyrrinda moraine (green) in the southern end of Bergsdalen.

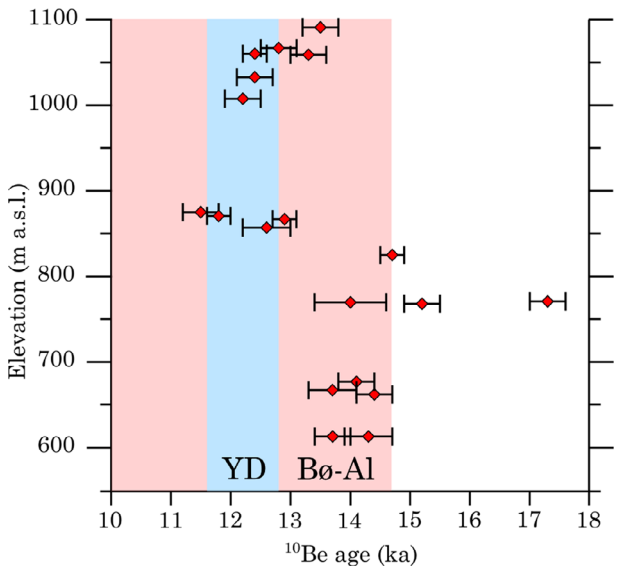

Fig. 9. ^{10}Be ages from the vertical transect on southern Ulvanosa (Fig. 8). Bølling-Allerød (Bø-Al), Younger Dryas (YD) and Holocene are marked for reference. Note YD ages at high elevations and older ages at lower elevations.

along this ridge and another four from the Dyrrinda moraine proper. The Dyrrinda samples yielded ages ranging from 14.4 to 10.5 ka. In addition to the oldest (14.4 ka) and the youngest (10.5 ka) ages, the other four ages are within 12.2–11.3 ka (Fig. 10), spanning the early Preboreal and late YD but with an average in the YD. The Dyrrinda moraine is the first moraine proximal to the lakes with undisturbed Allerød–YD sequences (see below), and thus a YD age is far more probable than a Preboreal age.

About 2 km south of the Dyrrinda moraine, across the mouth of Tveitdalen and only 400 m from the shore of Matersfjorden, lies a segmented moraine ridge (Fig. 10) that we consider to be a lateral moraine corresponding to the YD end moraine at the mouth of Matersfjorden (Fig. 6). On the distal side, i.e. north, of the moraine there are several glaciofluvial terraces located well above the marine limit (78 m a.s.l.), the largest being at 108–110 m a. s. l. and close to the moraine (Fig. 10). The high elevations suggest that these terraces were formed in ice-dammed lakes along the Matersfjorden glacier and that they were fed by a glacial river from the Dyrrinda moraine (Fig. 10). If correct, this supports the hypothesis that the Dyrrinda moraine was formed late in the YD.

Sediment cores and radiocarbon dating

To further investigate the extent of the YD ice sheet, we mapped the area between Ulvanosa and Matersfjorden and collected sediment cores from the three lakes Svartatjørna (314 m a.s.l.), Kleivahaugtjørn (240 m a.s.l.) and Langelivatnet (279 m a.s.l.) (Figs 3, 10). All three sediment cores were radiocarbon dated (Table 2).

Svartatjørna and Kleivahaugtjørn. – At Svartatjørna (Fig. 10) we cored from the floating fen surface surrounding the present lake. The corer stopped in coarse sediments, most likely till or glaciofluvial gravel, at 550 cm depth. The retrieved sediment succession (450–550 cm) displays six distinct units (Fig. 11). At the base is grey clayey silt with pebbles followed by 9 cm of brown gyttja. Above the gyttja is a 22-cm-thick, massive grey clayey silt including a 7-cm-thick Vedde Ash layer (12.1 cal. ka BP). Above the clayey silt is brown gyttja towards the top of the core, which represents typical Holocene lake sediments in western Norway. Four samples of plant macrofossils were extracted from the lower gyttja layer for AMS ^{14}C dating, resulted in ages between *c*. 12.9 and 13.5 cal. ka BP (Fig. 11). These ages suggest that the early Allerød is a minimum age for deglaciation, and that the area remained ice free throughout the YD.

Kleivahaugtjørn is a proglacial lake located distal from but adjacent to the Dyrrinda moraine ridge (Fig. 10). The coring stopped at 800 cm and revealed a similar sediment succession as in Svartatjørna (Fig. 11). The main difference is that in Kleivahaugtjørn the YD clayey layer above the Vedde Ash is much thicker and siltier and contains sand and pebbles (Fig. 11). We interpret this layer as resulting from the formation of the moraine ridge bordering the lake, and therefore that the Dyrrinda moraine was formed during the late YD (after the Vedde Ash, 12.1 ka). One radiocarbon date from the glacial sediments gave an age of *c*. 12.4 cal. ka BP but, as it is located above the Vedde Ash, we consider it as being derived from re-deposited organics. Three radiocarbon dates from the upper gyttja yielded, as expected, early Holocene ages with the lowermost one being 11.2 cal. ka BP (Fig. 11).

Lake Langelivatnet and the extent of the YD ice sheet in Matersfjorden. – As the stratigraphies in Svartatjørna and Kleivahaugtjørn (Fig. 11) as well as the ^{10}Be exposure ages show that the areas distal to the Dyrrinda moraine remained ice free throughout the YD, we wanted to map the YD extent of the Scandinavian Ice Sheet in this area.

At the southern end of Lake Langelivatnet, we identified a moraine ridge (Fig. 10) with a configuration suggesting that it was formed by an ice lobe filling the lake basin. The only possible source for such an ice lobe is the major outlet glacier filling the Matersfjorden (Fig. 6). On the valley side SW of Langelivatnet, the DTMs reveal an ~800 m long and narrow terrace at ~308 m a.s.l., i.e. ~30 m above the lake level (Figs 10, 12A). Smaller terraces were found at the corresponding elevation on the eastern valley side. As the valley in which Langelivatnet

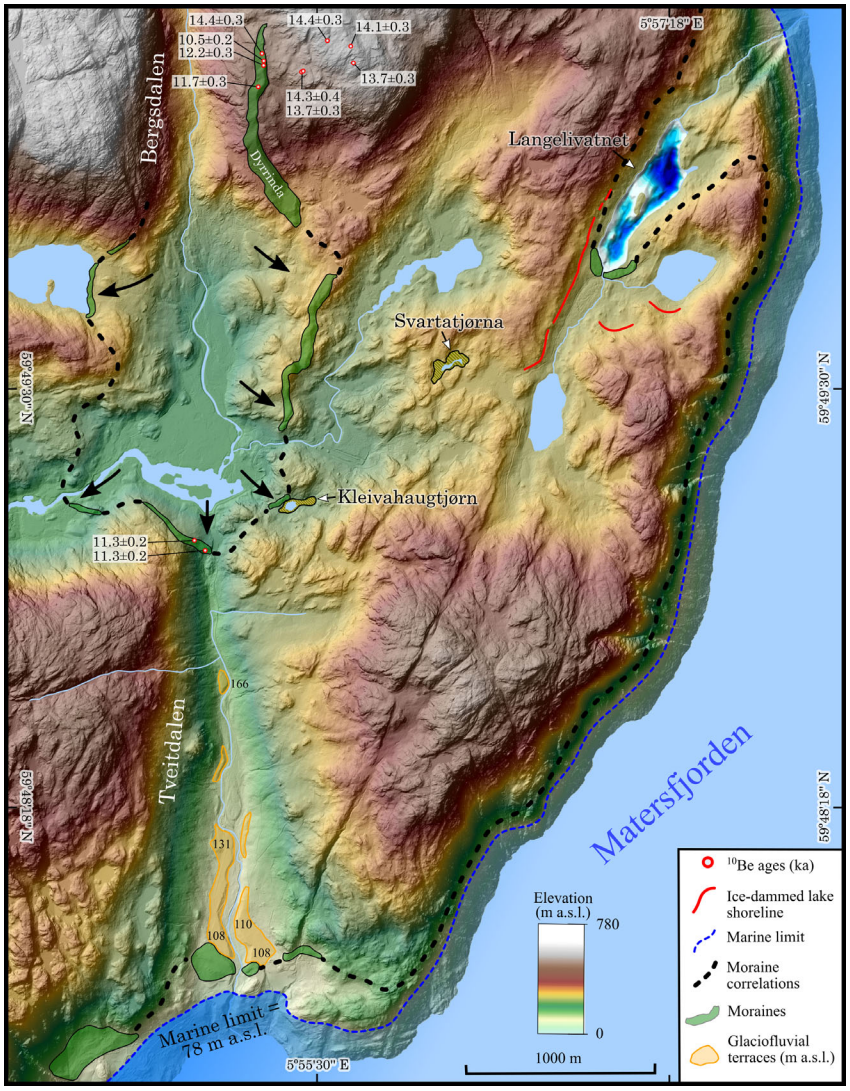

Fig. 10. Light Detection and Ranging (LiDAR) digital terrain model (DTM) of the area between Ulvanosa and Matersfjorden with ^{10}Be ages on and beyond the Dyrrinda moraine. Note the lobate continuation of the Dyrrinda moraine, the moraine and ice-dammed lake shoreline south of Lake Langelivatnet and the moraines and terraces in Tveitdalen.

resides currently drains northwards, we suggest that the terraces are shorelines formed in a lake dammed by the glacier tongue that formed the moraine south of Langelivatnet.

The bathymetric and seismic data revealed an undulating, high-amplitude reflection (acoustic basement), which we interpret as bedrock and/or a basal till, draped by acoustically layered sediments up to ~3 m in thickness (Fig. 12B). There were no signs of any moraine ridges on the lake floor, but point reflectors in the seismic record appearing just above the basement are interpreted as glacial boulders. The sediment core displays a simple stratigraphy with laminated clay and silt with intercalated sand layers in the lower 45 cm, followed by a sharp boundary to the overlying brown gyttja (Fig. 12D). The laminated silt and clay are interpreted as glaciolacustrine sediments deposited during ice-margin retreat from the lake basin. We assume that the deposition of the Holocene gyttja started soon after the ice margin retreated north of the valley and the inflow of glacial meltwater and sediments into Lake Langelivatnet stopped. Three radiocarbon dates from the lower part of the gyttja resulted in early Holocene ages, with the bottom two being *c.* 11.2 cal. ka BP (Fig. 12D), providing a minimum deglaciation age for Langelivatnet, and therefore also for the moraine ridge in its southern end.

Discussion

Emerging nunataqs and the onset of deglaciation

The oldest ^{10}Be exposure ages in this study, ranging from 155–18 ka, were obtained from the high mountain summits of Englafjell, Ulvanosa, Melderskind and

Table 2. Radiocarbon and Vedde Ash sample data and ages from Svartatjørna, Kleivahaugstjørn and Langelivatnet. Median ages are rounded to the nearest decade.

Depth (cm)	Weight (mg)	Weight C (mg)	Material	Laboratory ID	^{14}C ages (a BP)	Calibrated ages (cal. a BP)				
						68.2% confidence interval		95.4% confidence interval		Median
						From	To	From	To	
Svartatjørna										
524–525	2.4	1	*Betula nana* and *Salix* leaves	LuS 14482	10 970±60	12 767	12 961	12 760	13 065	12 890
527–528	2.6	1	Small stick	LuS 14483	11 750±60	13 505	13 741	13 493	13 758	13 600
531–532	2.7	1.2	Mixed plant remains	LuS 14484	11 410±60	13 183	13 333	13 168	13 419	13 280
532–533	1.7	0.4	Mixed plant remains	LuS 14485	11 605±70	13 363	13 577	13 319	13 594	13 460
511–518			The Vedde Ash			12 064±48	(Lohne *et al.* 2013, 2014)			
						12 121±57	(Rasmussen *et al.* 2006)[1]			
Kleivahaugstjørn										
729–730	13.9	1.3	Mixed plant remains	LuS 15345	8620±45	9534	9659	9528	9692	9590
741–742	1.7		Bulk sediment	LuS 15346	8855±50	9807	10 148	9730	10 172	9960
751–752	1.1		Bulk sediment	LuS 15347	9745±45	11 164	11 234	10 893	11 248	11 190
758–759	6.5	1.4	Mixed plant remains	LuS 15348	10 480±70	12 192	12 622	12 060	12 680	12 460
782–787			The Vedde Ash			12 064±48	(Lohne *et al.* 2013, 2014)			
						12 121±57	(Rasmussen *et al.* 2006)[1]			
Langelivatnet										
49	9.2	1.5	Small stick	LuS 15349	8330±45	9292	9427	9142	9471	9350
59–60	1.8		Bulk sediment	LuS 15350	9825±50	11 201	11 259	11 175	11 390	11 240
63–64	1.0		Bulk sediment	LuS 15351	9770±45	11 185	11 235	11 111	11 257	11 210

[1]This age is subtracted by 50 years from their B2K age in order to be comparable with calibrated ^{14}C ages.

Laurdalstind (Figs 5, 6). These ages may be used as arguments for the summits remaining ice free through LGM (e.g. Diesen 2003). However, we consider that the spread of the older ages, combined with the five much younger ages between 22 and 18 ka (Fig. 5), strongly suggests that the older ages are due to inheritance. Nuclide inheritance occurs when erratics (or bedrock) have been exposed during previous ice-free periods, or if the parent bedrock has not been sufficiently eroded (>2 m) to remove previously produced ^{10}Be, resulting in apparent ages older than the time of deglaciation (e.g. Briner *et al.* 2005). Several studies have demonstrated that inheritance increases with altitude in Norway (Egholm *et al.* 2017; Andersen *et al.* 2018; Jansen *et al.* 2019). We therefore conclude that the oldest ages are due to inheritance. We also conclude that the youngest ages show that all summits were ice covered during the LGM, and protruded as nunataqs *c.* 22–18 ka. However, owing to the inheritance, and indeed other sources of error, we do not consider the face values of these ages as very reliable.

The age range of 21–18 ka overlaps with age estimates (20–18.5 ka) of the shut down and subsequent break-up of the Norwegian Channel Ice Stream (Lehman *et al.* 1991; Sejrup *et al.* 1994, 2016; King *et al.* 1998; Svendsen *et al.* 2015; Morén *et al.* 2018). We acknowledge the low precision in the age determinations for both events, but we postulate that the retreat of the ice-stream margin would result in a lowering of the ice-sheet surface over Hardangerfjorden and thus the first emergence of the higher mountain summits as nunataqs (Fig. 13).

Deglaciation from the outer coast

At the westernmost locality, the summit of mount Siggjo, the ^{10}Be ages grouped around 14.5 ka (after removal of an outlier of 6.1 ka), and thus overlap with previous ^{10}Be ages from lower elevations on southern Bømlo (Mangerud *et al.* 2013) and from Ryvarden south of Bømlo (Gump *et al.* 2017) (Fig. 13). The similar ages obtained near sea level and on summits along the outer coast suggest such a fast retreat/thinning that the time differences are within the uncertainties of the method, as also shown slightly farther north (Mangerud *et al.* 2017). A main point is that following deglaciation of the Norwegian Channel, at *c.* 20–18.5 ka, there was little or no ice-sheet retreat until *c.* 14.5 ka, when the mouth of Hardangerfjorden became ice free, again a parallel situation to the adjacent area to the north (Mangerud *et al.* 2017). We suggest that the halt in ice recession following the collapse of the Norwegian Ice Stream is due to the many islands along the coast and the shallow sill at the mouth of Hardangerfjorden and other fjords (Fig. 13) acting as pinning points that stabilized the ice

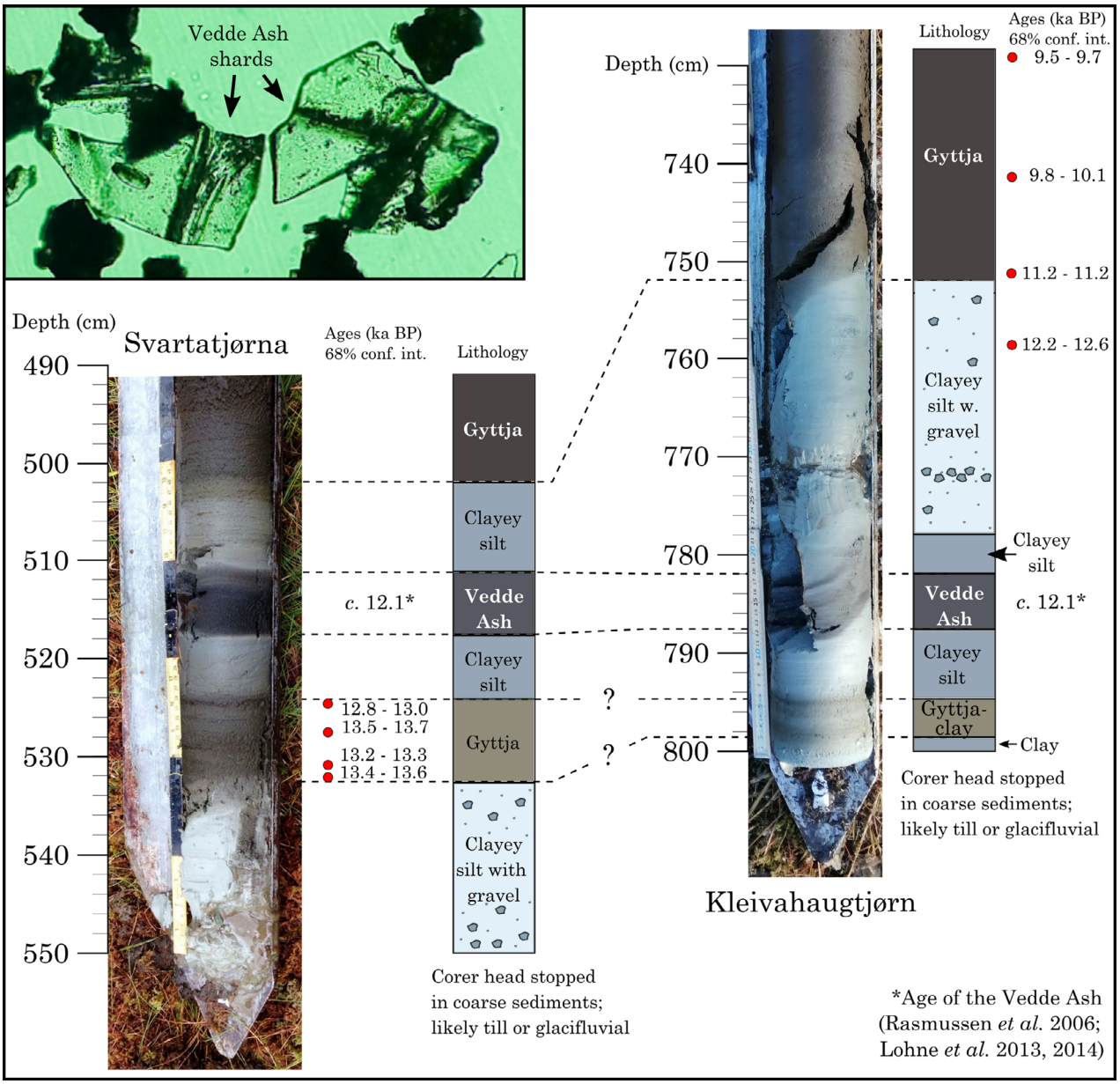

Fig. 11. Photographs and lithological logs of sediment cores from Svartatjørna (314 m a.s.l.) and Kleivahaugtjørn (240 m a.s.l.) (locations in Fig. 10), as well as a microscope image (top left) of <1 mm Vedde Ash shards from the Svartatjørna core. Correlations between the two cores are marked by dashed lines. Note the much thicker and coarser minerogenic layer, interpreted as a glacial signal, above the Vedde Ash in Kleivahaugtjørn compared with Svartatjørna. As both cores contain undisturbed Allerød–YD sediments, they show that the sites remained ice free throughout the YD (see Fig. 14).

margin. ^{10}Be ages from Boknafjorden slightly farther south (Fig. 2A) suggest that its deglaciation initiated as early as *c.* 16 ka (Fig. 2; Svendsen *et al.* 2015; Gump *et al.* 2017), i.e. some 1500 years before the mouth of Hardangerfjorden. The earlier deglaciation of Boknafjorden is potentially due to the absence of pinning points in its deep and wide trough (>200 m depth and >8 km width).

Following deglaciation from the outer coast at *c.* 14.5 ka, the ice margin retreated fast during the mild Bølling period and was located inside the Halsnøy moraine after only a few hundred years (Mangerud *et al.* 2016). However, the retreat in Bølling was interrupted by an Older Dryas re-advance, reaching past the YD position. The Older Dryas re-advance is suggested based on Bølling ages of shell fragments in tills both outside and inside the YD moraine (Mangerud *et al.* 2016). Contrastingly, in the Bergen area, slightly to the north, the Older Dryas ice margin is interpreted as being located inland of the YD margin (Mangerud *et al.* 2017). However, when studying

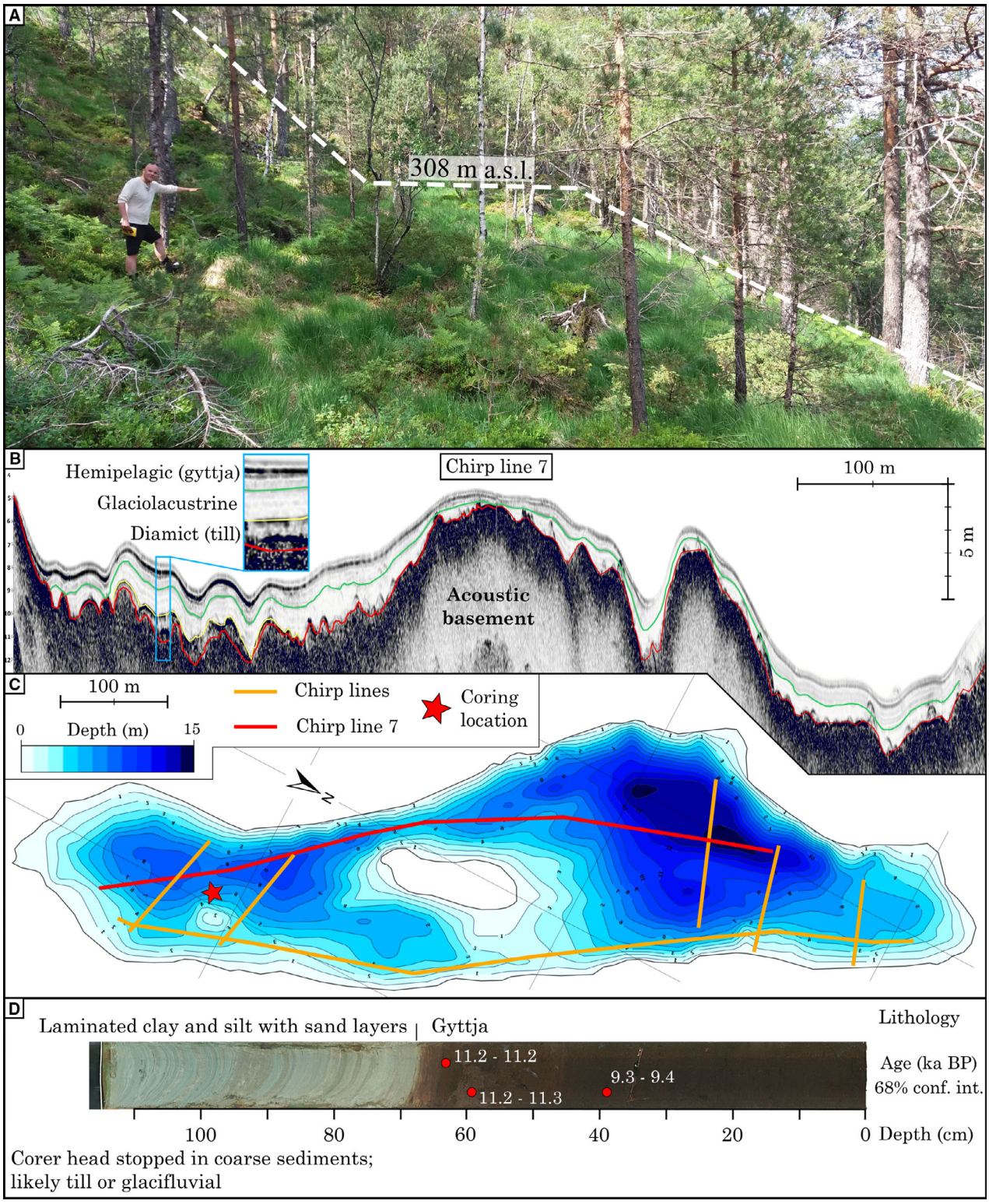

Fig. 12. A. Photograph of the ice-dammed lake shoreline south of Langelivatnet (photograph, Reidun Eldegard). B. Chirp line 7 from Langelivatnet (red line in D) and lithological interpretation of reflectors. C. Bathymetric map of Langelivatnet with chirp lines and coring location. D. Sediment core with radiocarbon dates (coring location marked in C).

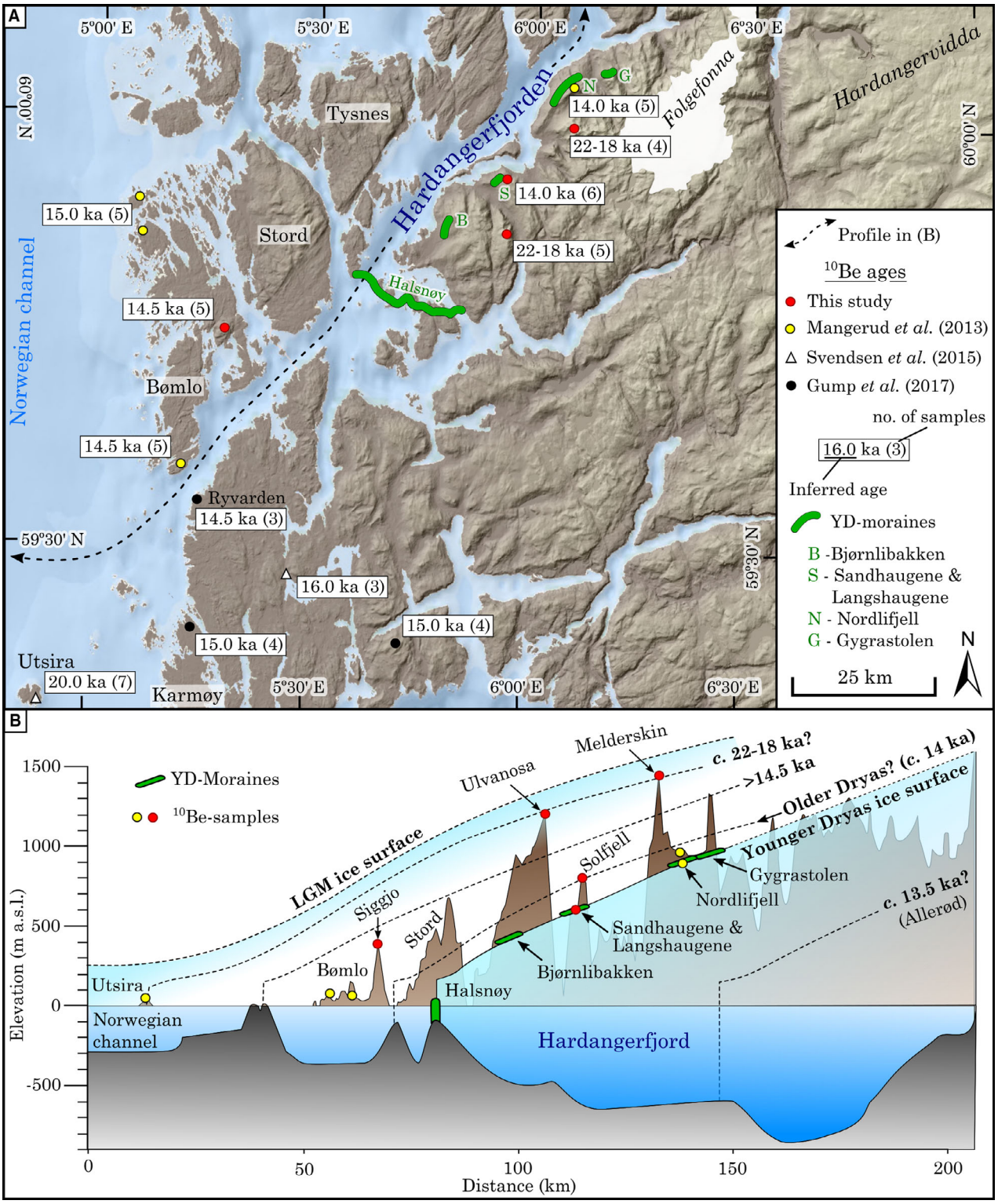

Fig. 13. A. ^{10}Be ages from outside and above the Younger Dryas moraines. Ages are rounded to nearest 0.5 ka. The Younger Dyas moraines shown in (B) are marked in green. B. Topographic profile from the Norwegian channel in the SW to inner Hardangerfjorden in the NE (location of the profile shown in A). Ice-sheet profiles based on our interpretations are shown for key time slices discussed in the text.

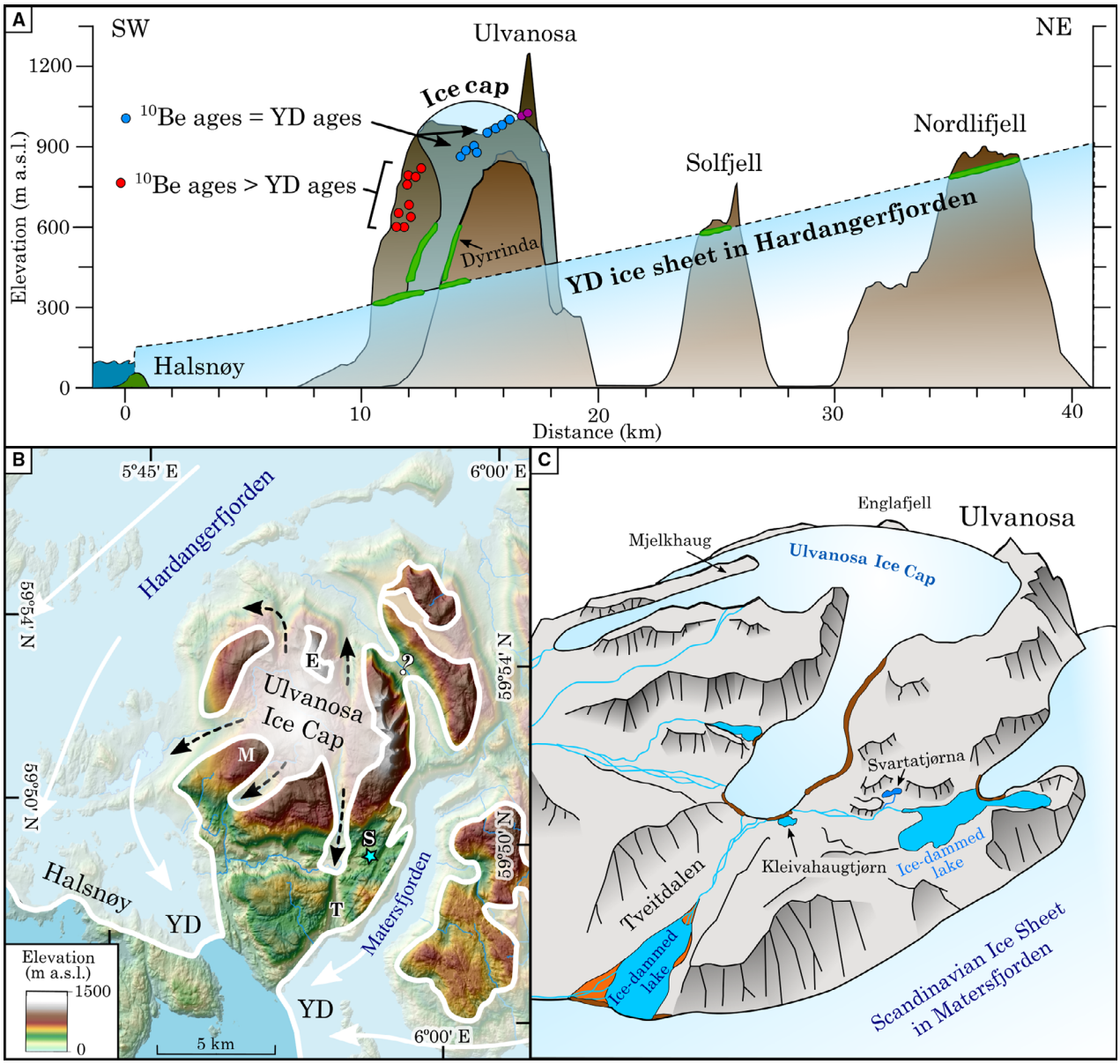

Fig. 14. Our main interpretations of the YD-ice extent in the area. A. Topographic profile of outer Hardangerfjorden with the Younger Dryas ice surface. Note the ^{10}Be samples from high elevations on Ulvanosa, yielding Younger Dryas ages, and the high elevation of the Dyrrinda moraine, consistent with our interpretation of the Dyrinda moraine as formed by a local ice cap and dated to the late YD. B. Reconstruction of the Younger Dryas ice extent, where we postulate an independent ice cap on the Ulvanosa massif. The locations of M = Mjelkhaug, E = Englafjell, T = Tveitdalen and S = Svartatjørna are marked. C. Schematic 3D reconstruction of the Younger Dryas ice cap on the Ulvanosa massif seen from Matersfjorden towards north.

LiDAR DTMs of areas surrounding the outer part of Hardangerfjorden, we did not find any ice-marginal landforms outside of the YD moraines, but we note that there is a shallow threshold in Hardangerfjorden between Bømlo and Stord (Fig. 13B) that potentially acted as a pinning point for the ice sheet, resulting in a temporary halt in retreat or the end of a re-advance. Unfortunately, the large spread and uncertainties of our ^{10}Be ages from sites just outside and above the YD moraines (outside the Dyrrinda moraine, Fig. 10, and on top of Solfjell, Fig. 6) span across the Older Dryas, and thus cannot provide a conclusive answer as to whether these sites were deglaciated prior to or after the Older Dryas. However, the basal dates of *c.* 13.5 cal. ka of the Svartatjørna sediment core (Fig. 9) indicate that this area was deglaciated after the Older Dryas, suggesting a more extensive ice cover there during the Older Dryas than the YD. Following 14 ka, the ice margin in Hardangerfjorden retreated at least another 80 km during the Allerød before it re-advanced at least 60 km to its YD maximum position at the Halsnøy moraine (Figs 2A, 13B; Mangerud *et al.* 2016).

The Younger Dryas ice sheet and a local ice cap between Hardangerfjorden and Matersfjorden

The culmination of the ice-sheet re-advance in Hardangerfjorden, at the Halsnøy moraine, is dated to the very end of the YD; 11.8 to 11.6 cal. ka BP (Lohne *et al.* 2012). In earlier reconstructions (e.g. Follestad 1972) it was assumed that the YD ice sheet inundated the entire area between Hardangerfjorden and Matersfjorden (Figs 2A, 3). However, the pre-YD ^{10}Be ages from the lower end of our dating transect at Ulvanosa (Figs 8, 9), together with the undisturbed sediment successions across the YD from Svartatjørna and Kleivahaugtjørn (Fig. 11), show that these areas instead remained ice free throughout the YD. The Matersfjorden outlet glacier from the Scandinavian Ice Sheet must, therefore, have been confined to lower elevations along the fjord with only a smaller glacier tongue reaching up across Lake Langelivatnet (Figs 10, 14).

A Younger Dryas ice cap on the Ulvanosa massif and the age of the Dyrrinda moraine. – The YD ^{10}Be ages from high elevations (~850–1100 m a.s.l.) on the Ulvanosa mountain massif (Figs 8, 9) suggest that parts of this mountain were covered by ice during the YD. On the other hand, the pre-YD ^{10}Be ages and sediment stratigraphies from the lower areas (Fig. 11) demonstrate that the ice sheet did not reach this high during the YD. The interpretation must be that there was an independent ice cap on Ulvanosa during the YD (Fig. 14) and that the Dyrrinda moraine represents an outlet glacier from this ice cap.

Unfortunately, given the spread and uncertainty of the ^{10}Be ages from the Dyrrinda moraine, they span both the early Preboreal and late YD and cannot alone provide a conclusive age of moraine formation. Likewise, the sediment stratigraphy from Kleivahaugtjørn (Fig. 11) can only constrain the age of the Dyrrinda moraine to sometime between 12.1 and 11.2 cal. ka BP from numerical dates.

The highest elevation of a lateral moraine is a measure of the minimum height of the Equilibrium Line Altitude (ELA) (Andersen 1954), and in practice it is often a good approximation of the ELA (e.g. Larsen *et al.* 1984). The Dyrrinda moraine can be traced to 575 m a.s.l., or ~500 m above the YD sea level, which fits well with the tilted late YD-ELA in Mangerud *et al.* (2016). In addition, a late YD age of the Dyrrinda moraine is supported by the correlation with the glaciofluvial terraces in Tveitdalen (Fig. 10). A minimum age for the terraces is the time when this part of Matersfjorden was finally deglaciated, which can be obtained by dating the marine limit terrace (78 m a.s.l.) at the mouth of Tveitdalen. When plotting this elevation onto the master shoreline diagram for western Norway (Mangerud *et al.* 2019), it yields an age of *c.* 11.4 cal. ka BP, consistent with ice-margin retreat from the Halsnøy moraine at 11.6 cal. ka BP (Lohne *et al.* 2012). Thus, the age of the Dyrrinda moraine is bracketed between 12.1 (the Vedde Ash at Kleivahaugtjørn) and 11.4 cal. ka BP. We therefore conclude that the Ulvanosa Ice Cap reached its maximum extent in concert with the ice sheet in Hardangerfjorden (Lohne *et al.* 2012), i.e at the very end of the YD, after which it retreated at the onset of the Holocene.

Conclusions

- The higher mountain summits in the outer Hardangerfjorden area (~1200–1400 m a.s.l.) were ice covered during the LGM and melted out as nunataqs *c.* 22–18 ka, probably as a consequence of the break-up of the Norwegian Channel Ice Stream.
- Following break-up of the Norwegian Channel Ice Stream, the ice margin stabilized at the outermost coast for 3500–5500 years, before the mouth of Hardangerfjorden deglaciated at *c.* 14.5 ka.
- More extensive areas that were ice free during the YD, which earlier were considered ice covered, are documented between Hardangerfjorden and Matersfjorden.
- We discovered that there has been a local 'Ulvanosa Ice Cap' on mountains adjacent to the outer Hardangerfjorden during the YD. It was independent of the Scandinavian Ice Sheet but feeding into it on the north flank.
- The Ulvanosa Ice Cap reached its maximum extent during late YD, simultaneously with the ice sheet in Hardangerfjorden.
- The ELA for the Ulvanosa Ice Cap is consistent with an inland-rising ELA values reported in prior studies.

Acknowledgements. – This study is a contribution to the projects Climate History along the Arctic Seaboard of Eurasia 'CHASE' (NRC 255415, Research Council of Norway), Eurasian Ice Sheet and Climate Interactions: Reconstructing and modelling the climate and ice sheet evolution of the last glacial cycle 'EISCLIM' (NRC 229788, Research Council of Norway) and the RISES Project on Quantifying and understanding rates of ice sheet change, Bjerknes Centre for Climate Research. We thank Eivind Støren, Johannes Hardeng, Reidun Eldegard, Fredrik Hjort Karlsen, Ole Tvedt, Kjell Tore Holmdal and Olav Sæbo for their help during fieldwork. Gunhild 'Ninis' Rosqvist and Gifford H. Miller are thanked for discussions and comments on an earlier version of this paper. We also thank the two reviewers, T. Lane and E. Larsen, for their valuable comments on the manuscript, which helped improve it.

Author contributions. – This project was initiated by JIS and JM, and much of the ^{10}Be rock sampling field work was performed prior to CR started on his Ph.D. project. CR performed much of the subsequent field work (all sediment coring and additional rock sampling), did the remote sensing analyses, conducted laboratory analyses of the sediment cores and wrote the first draft of the manuscript, but all authors participated in formulations and modifications. JIS was project leader and participated in all field work. JM participated in developing the ideas and in most of the field work. HH participated in field work and analyses concerning sediment cores and seismics. JB participated in some field work (rock sampling) and conducted all ^{10}Be analyses.

Data availability statement. – Additional chirp lines from Langelivatnet not shown here are available from the lead author upon request.

References

Aarseth, I. 1997: Western Norwegian fjord sediments: age, volume, stratigraphy, and role as temporary depository during glacial cycles. *Marine Geology 143*, 39–53.

Åkesson, H., Gyllencreutz, R., Mangerud, J., Svendsen, J. I., Nick, F. M. & Nisancioglu, K. H. 2020: Rapid retreat of a Scandinavian marine outlet glacier in response to warming at the last glacial termination. *Quaternary Science Reviews 250*, 106645, https://doi.org/10.1016/j.quascirev.2020.106645.

Andersen, B. G. 1954: Randmorener i Sørvest-Norge. *Norsk Geografisk Tidsskrift - Norwegian Journal of Geography 14*, 273–342.

Andersen, J. L., Egholm, D. L., Knudsen, M. F., Linge, H., Jansen, J. D., Pedersen, V. K., Nielsen, S. B., Tikhomirov, D., Olsen, J., Fabel, D. & Xu, S. 2018: Widespread erosion on high plateaus during recent glaciations in Scandinavia. *Nature Communications 9*, 830, https://doi.org/10.1038/s41467-018-03280-2.

Anundsen, K. 1972: Glacial chronology in parts of southwestern Norway. *Norges Geologiske Undersøkelse 280*, 1–24.

Balco, G. 2017: Production rate calculations for cosmic-ray-muon-produced ^{10}Be and ^{26}Al benchmarked against geological calibration data. *Quaternary Geochronology 39*, 150–173.

Balco, G., Stone, J. O., Lifton, N. A. & Dunai, T. J. 2008: A complete and easily accessible means of calculating surface exposure ages or erosion rates from ^{10}Be and ^{26}Al measurements. *Quaternary Geochronology 3*, 174–195.

Borchers, B., Marrero, S., Balco, G., Caffee, M., Goehring, B., Lifton, N., Nishiizumi, K., Phillips, F., Schaefer, J. & Stone, J. 2015: Geological calibration of spallation production rates in the CRONUS-Earth project. *Quaternary Geochronology 31*, 188–198.

Briner, J. P., Goehring, B. M., Mangerud, J. & Svendsen, J. I. 2016: The deep accumulation of ^{10}Be at Utsira, southwestern Norway: Implications for cosmogenic nuclide exposure dating in peripheral ice sheet landscapes. *Geophysical Research Letters 43*, 9121–9129.

Briner, J. P., Miller, G. H., Davis, P. T. & Finkel, R. C. 2005: Cosmogenic exposure dating in arctic glacial landscapes: implications for the glacial history of northeastern Baffin Island, Arctic Canada. *Canadian Journal of Earth Sciences 42*, 67–84.

Brook, E. J., Nesje, A., Lehman, S. J., Raisbeck, G. M. & Yiou, F. 1996: Cosmogenic nuclide exposure ages along a vertical transect in western Norway: Implications for the height of the Fennoscandian ice sheet. *Geology 24*, 207–210.

Clark, P. U., Dyke, A. S., Shakun, J. D., Carlson, A. E., Clark, J., Wohlfarth, B., Mitrovica, J. X., Hostetler, S. W. & McCabe, A. M. 2009: The Last Glacial Maximum. *Science 325*, 710–714.

Diesen, M. G. 2003: *Den vertikale isutbredelse i Kvinnherad under siste istid*. Hovedoppgave i kvartærgeologi, Department of Earth Science, University of Bergen, 133 pp.

Egholm, D. L., Jansen, J. D., Brædstrup, C. F., Pedersen, V. K., Andersen, J. L., Ugelvig, S. V., Larsen, N. K. & Knudsen, M. F. 2017: Formation of plateau landscapes on glaciated continental margins. *Nature Geoscience 10*, 592–597.

Fjeldskaar, W. 2000: An isostatic test of the hypothesis of ice-free mountain areas during the last glaciation. *Norsk Geologisk Tidsskrift 80*, 51–56.

Follestad, B. A. 1972: The deglaciation of the south-western part of the Folgefonn peninsula. *Norges Geologiske Undersøkelse 280*, 31–64.

Follestad, B. A. 1990: Block fields, ice-flow directions and the Pleistocene ice sheet in Nordmore and Romsdal, West Norway. *Norsk Geologisk Tidsskrift 70*, 27–33.

Goehring, B. M., Brook, E. J., Linge, H., Raisbeck, G. M. & Yiou, F. 2008: Beryllium-10 exposure ages of erratic boulders in southern Norway and implications for the history of the Fennoscandian Ice Sheet. *Quaternary Science Reviews 27*, 320–336.

Goehring, B. M., Lohne, Ø. S., Mangerud, J., Svendsen, J. I., Gyllencreutz, R., Schaefer, J. & Finkel, R. 2012a: Late glacial and Holocene ^{10}Be production rates for western Norway. *Journal of Quaternary Science 27*, 89–96.

Goehring, B. M., Lohne, Ø. S., Mangerud, J., Svendsen, J. I., Gyllencreutz, R., Schaefer, J. & Finkel, R. 2012b: Erratum: Late glacial and Holocene ^{10}Be production rates for western Norway. *Journal of Quaternary Science 27*, 89–96.

Gump, D. J., Briner, J. P., Mangerud, J. & Svendsen, J. I. 2017: Deglaciation of Boknafjorden, south-western Norway. *Journal of Quaternary Science 32*, 80–90.

Holtedahl, H. 1967: Notes on the Formation of Fjords and Fjord-Valleys. *Geografiska Annaler: Series A, Physical Geography 49*, 188–203.

Holtedahl, H. 1975: The geology of Hardangerfjord, west Norway. *Norges Geologiske Undersøkelse 323*, 1–87.

Hughes, A. L. C., Gyllencreutz, R., Lohne, Ø. S., Mangerud, J. & Svendsen, J. I. 2016: The last Eurasian ice sheets - a chronological database and time-slice reconstruction, DATED-1. *Boreas 45*, 1–45.

Jansen, J. D., Knudsen, M. F., Andersen, J. L., Heyman, J. & Egholm, D. L. 2019: Erosion rates in Fennoscandia during the past million years. *Quaternary Science Reviews 207*, 37–48.

Jones, R. S., Whitehouse, P. L., Bentley, M. J., Small, D. & Dalton, A. S. 2019: Impact of glacial isostatic adjustment on cosmogenic surface-exposure dating. *Quaternary Science Reviews 212*, 206–212.

King, E., Haflidason, H., Sejrup, H. P. & Løvlie, R. 1998: Glacigenic debris flows on the North Sea Trough Mouth Fan during ice stream maxima. *Marine Geology 152*, 217–246.

Lal, D. 1991: Cosmic ray labeling of erosion surfaces: in situ nuclide production rates and erosion models. *Earth and Planetary Science Letters 104*, 424–439.

Larsen, E., Eide, F., Longva, O. & Mangerud, J. 1984: Allerød-Younger Dryas Climatic Inferences from Cirque Glaciers and Vegetational Development in the Nordfjord Area, Western Norway. *Arctic and Alpine Research 16*, 137–160.

Lehman, S. J., Jones, G. A., Keigwin, L. D., Andersen, E. S., Butenko, G. & Østmo, S. R. 1991: Initiation of Fennoscandian ice-sheet retreat during the last deglaciation. *Nature 349*, 513–516.

Lohne, Ø. S., Bondevik, S., Mangerud, J. & Svendsen, J. I. 2007: Sea-level fluctuations imply that the Younger Dryas ice-sheet expansion in western Norway commenced during the Allerød. *Quaternary Science Reviews 26*, 2128–2151.

Lohne, Ø. S., Mangerud, J. & Birks, H. H. 2013: Precise ^{14}C ages of the Vedde and Saksunarvatn ashes and the Younger Dryas boundaries from western Norway and their comparison with the Greenland Ice Core (GICC05) chronology. *Journal of Quaternary Science 28*, 490–500.

Lohne, Ø. S., Mangerud, J. & Birks, H. H. 2014: IntCal13 calibrated ages of the Vedde and Saksunarvatn ashes and the Younger Dryas boundaries from Kråkenes, western Norway. *Journal of Quaternary Science 29*, 506–507.

Lohne, Ø. S., Mangerud, J. & Svendsen, J. I. 2012: Timing of the Younger Dryas glacial maximum in western Norway. *Journal of Quaternary Science 27*, 81–88.

Mangerud, J. 2000: Was Hardangerfjorden, western Norway, glaciated during the Younger Dryas? *Norsk Geologisk Tidsskrift 80*, 229–234.

Mangerud, J., Aarseth, I., Hughes, A. L. C., Lohne, Ø. S., Skår, K., Sønstegaard, E. & Svendsen, J. I. 2016: A major re-growth of the Scandinavian Ice Sheet in western Norway during Allerød-Younger Dryas. *Quaternary Science Reviews 132*, 175–205.

Mangerud, J., Briner, J. P., Goslar, T. & Svendsen, J. I. 2017: The Bølling-age Blomvåg Beds, western Norway: implications for the Older Dryas glacial re-advance and the age of the deglaciation. *Boreas 46*, 162–184.

Mangerud, J., Goehring, B. M., Lohne, Ø., Svendsen, J. I. & Gyllencreutz, R. 2013: Collapse of marine-based outlet glaciers from the Scandinavian Ice Sheet. *Quaternary Science Reviews 67*, 8–16.

Mangerud, J., Hughes, A. L. C., Sæle, T. H. & Svendsen, J. I. 2019: Ice-flow patterns and precise timing of ice sheet retreat across a dissected fjord landscape in western Norway. *Quaternary Science Reviews 214*, 139–163.

Mangerud, J., Larsen, E., Longva, O. & Sønstegaard, E. 1979: Glacial history of western Norway 15,000–10,000 B.P. *Boreas 8*, 179–187.

Mangerud, J., Lie, S. E., Furnes, H., Kristiansen, I. L. & Lømo, L. 1984: A Younger Dryas ash bed in western Norway, and its possible correlations with tephra in cores from the Norwegian Sea and the North Atlantic. *Quaternary Research 21*, 85–104.

Morén, B. M., Sejrup, H. P., Hjelstuen, B. O., Borge, M. V. & Schäuble, C. 2018: The last deglaciation of the Norwegian Channel – geomorphology, stratigraphy and radiocarbon dating. *Boreas 47*, 347–366.

Nesje, A. 1992: A piston corer for lacustrine and marine sediments. *Arctic and Alpine Research 24*, 257–259.

Nesje, A., Anda, E., Rye, N., Lien, R., Hole, P. A. & Blikra, L. H. 1987: The vertical extent of the Late Weichselian ice sheet in the Nordfjord-Møre area, western Norway. *Norsk Geografisk Tidsskrift 67*, 125–141.

Nesje, A. & Dahl, S. O. 1990: Autochthonous block fields in southern Norway: Implications for the geometry, thickness, and isostatic loading of the Late Weichselian Scandinavian ice sheet. *Journal of Quaternary Science 5*, 225–234.

Nesje, A., Dahl, S. O., Anda, E. & Rye, N. 1988: Block fields in southern Norway: significance for the Late Weichselian ice sheet. *Norsk Geologisk Tidsskrift 68*, 149–169.

Nishiizumi, K., Imamura, M., Caffee, M. W., Southon, J. R., Finkel, R. C. & McAninch, J. 2007: Absolute calibration of ^{10}Be AMS standards. *Nuclear Instruments and Methods in Physics Research Section B: Beam Interactions with Materials and Atoms 258*, 403–413.

Rasmussen, S. O., Andersen, K. K., Svensson, A. M., Steffensen, J. P., Vinther, B. M., Clausen, H. B., Siggaard-Andersen, M. L., Johnsen, S. J., Larsen, L. B., Dahl-Jensen, D., Bigler, M., Röthlisberger, R., Fischer, H., Goto-Azuma, K., Hansson, M. E. & Ruth, U. 2006: A new Greenland ice core chronology for the last glacial termination. *Journal of Geophysical Research Atmospheres 111*, D06102, https://doi.org/10.1029/2005JD006079.

Reimer, P. J. & 41 others 2020: The IntCal20 Northern Hemisphere Radiocarbon Age Calibration Curve (0–55 cal kBP). *Radiocarbon 62*, 725–757.

Rood, D. H., Hall, S., Guilderson, T. P., Finkel, R. C. & Brown, T. A. 2010: Challenges and opportunities in high-precision Be-10 measurements at CAMS. *Nuclear Instruments and Methods in Physics Research Section B: Beam Interactions with Materials and Atoms 268*, 730–732.

Sejrup, H. P., Clark, C. D. & Hjelstuen, B. O. 2016: Rapid ice sheet retreat triggered by ice stream debuttressing: Evidence from the North Sea. *Geology 44*, 355–358.

Sejrup, H. P., Haflidason, H., Aarseth, I., King, E., Forsberg, C. F., Long, D. & Rokoengen, K. 1994: Late Weichselian glaciation history of the northern North Sea. *Boreas 23*, 1–13.

Sollid, J. L. & Sørbel, L. 1994: Distribution of glacial fandforms in southern Norway in relation to the thermal regime of the last continental ice sheet. *Geografiska Annaler: Series A, Physical Geography 76*, 25–35.

Staiger, J., Gosse, J., Toracinta, R., Oglesby, B., Fastook, J. & Johnson, J. V. 2007: Atmospheric scaling of cosmogenic nuclide production: Climate effect. *Journal of Geophysical Research 112*, B02205. https://doi.org/10.1029/2005JB003811.

Stroeven, A. P., Heyman, J., Fabel, D., Björck, S., Caffee, M. W., Fredin, O. & Harbor, J. M. 2015: A new Scandinavian reference ^{10}Be production rate. *Quaternary Geochronology 29*, 104–115.

Svendsen, J. I., Briner, J. P., Mangerud, J. & Young, N. E. 2015: Early break-up of the Norwegian Channel Ice Stream during the Last Glacial Maximum. *Quaternary Science Reviews 107*, 231–242.

Undås, I. 1963: *Ra-morenen i Vest-Norge*. 78 pp. J.W. Eides forlag A.S., Bergen.

Vasskog, K., Svendsen, J., Mangerud, J., Agasøster Haaga, K., Svean, A. & Lunnan, E. M. 2019: Evidence of early deglaciation (18 000 cal a BP) and a postglacial relative sea-level curve from southern Karmøy, south-west Norway. *Journal of Quaternary Science 34*, 410–423.

Young, N. E., Briner, J. P., Rood, D. H., Finkel, R. C., Corbett, L. B. & Bierman, P. R. 2013: Age of the Fjord Stade moraines in the Disko Bugt region, western Greenland, and the 9.3 and 8.2 ka cooling events. *Quaternary Science Reviews 60*, 76–90.